RSC Advances

ROYAL SOCIETY OF CHEMISTRY

www.rsc.org/advances

High Thermal Conductivity and High Impact Strength of Epoxy Nanodielectrics with Functionalized Halloysite Nanotubes

Hailin Mo[a], Ke Yang[a], Shengtao Li[b] and Pingkai Jiang*[a]

[a]*Department of Polymer Science and Engineering and Shanghai Key Lab of Electrical Insulation and Thermal Aging, Shanghai Jiao tong University, 200240 Shanghai, China. E-mail pkjiang@sjtu.edu.cn; Tel 86-021-54746520*

[b]*State Key Lab of electrical Insulation and Power Equipment, Xi'an Jiaotong University, Xi'an, China*

Keywords: high thermal conductive, in-situ grafted Halloysite Nanotubes, Nanodielectric Materials, excellent dielectric properties, high impact strength

Abstract:

Epoxy nanodielectrics with high thermal conductivity and high impact strength have become the increasingly desirable material of electronic and electric industries. In this paper, three functionalized Halloysite Nanotubes (HNTs) named p-HNTs (treated by KH 560), b-HNTs (in-situ grafted by benzidine) and d-HNTs (in-situ grafted by 4, 4'-(1, 1'-biphenyl-4, 4'-diyidioxy) dianiline) were used to fabricate thermally conductive epoxy/HNTs nanodielectrics with high impact strength. It was found that the surface modification of HNTs play very important roles in enhance the mechanical, thermal and dielectric properties of epoxy nanodielectrics. The obtained epoxy/b-HNTs nanodielectrics with 60 wt. % filler presented the highest

thermal conductivity of 0.85 W m^{-1} K^{-1} (about 30% higher than that of epoxy/HNTs nanodielectrics). The impact strength of epoxy/b-HNTs nanodielectrics is about 5.8 kJ m^{-2}, 1.5 times that of epoxy/HNTs nanodielectrics. The epoxy/b-HNTs nanodielectrics also possessed excellent thermal stability and electrical insulation properties. In summary, the epoxy epoxy/b-HNTs nanodielectrics showed the best overall performance among all epoxy thermosets/in-situ grafting HNTs. The results of SEM images showed that the improved physical properties of epoxy nanodielectrics were attributed to the increased interaction between in-situ grafted HNTs and epoxy matrix and better dispersion of the in-situ grafted HNTs in epoxy matrix. The results suggested that the obtained epoxy nanodielectrics might be promising as efficient heat-releasing materials for thermal management and next generation electronic devices.

Keywords: epoxy nanodielectrics, impact strength, thermal conductivity, Halloysite nanotubes (HNTs)

1. Introduction

The amino epoxy resins are widely used nowadays as the preferred matrix materials

for high performance carbon fiber composites in power grid system, aerospace, missiles and spacecraft due to their excellent heat resistance, nice dielectric property and desirable processability.[1-4] However, the drawbacks of the inferior impact strength and low thermal conductive have greatly restricted their many applications. Although there are a few attempts made to improve the fracture toughness of the amino epoxy resins, [5, 6] it is still hard to balance its toughness and high performance. Many practical applications and researches introduced plasticizers [6], liquid rubbers [7], rigid inorganic additives and high-performance engineering thermoplastics [8-12] to bisphenol A epoxy matrix for epoxy toughening. The strategies used in the bisphenol A epoxy resins are still the effective ways to modify the fracture toughness of the amino epoxy resins. However, the achievement of the above strategies depended on solving the major drawbacks, which were the decrease in the modulus, strength and thermal properties, [13] the difficulty in controlling interface compatibility of epoxy/additives and the bad toughening efficiency of the rigid inorganic additives. These drawbacks limited their applications in many fields requiring high thermal conductivity and high impact strength.

Over the past decades, considerable progress has been made to improve the thermal conductive of epoxy thermosets by synthetizing the novel epoxy resins [14, 15] and preparing the epoxy/nanoparticles nanodielectrics filled with the thermal conductivity nanoparticles.[16-18] However, preparing an amino epoxy nanodielectrics

with the high thermal conductive and high impact strength is still a matter of research.

Halloysite nanotubes (HNTs) are the type of naturally occurring clay with an elongated hollow nanotubular structure and a large aspect ratio.[19, 20] HNTs have attracted a great deal of attentions for a promising reinforcing filler of epoxy thermosets with high impact strength.[21, 22] The considerable results of prior researches demonstrate that the blending epoxies with an appropriate amount of HNTs can noticeably improve the fracture toughness, impact strength and the storage modulus without sacrificing their thermal mechanical properties.[21-25] And the underlying toughening mechanisms were also identified as massive micro-cracking, nanotube bridging/pull-out/breaking and crack deflection.[21,22] However, HNTs have large specific surface area, high van de Walls force and low concentration of polar functional groups on the external surface, this properties lead to poor dispersion and weak interfacial interaction in epoxy/HNTs matrix, which deteriorate the mechanical properties of the epoxy nanodielectrics.[26-31] Although the chemical functionalization of HNTs is considered as one of the most easy ways among the various methods to apply in designing a good compatibility toward to epoxy resins, as well as other physicochemical properties,[31-33] the mass production in term of quantity, quality and cost has been one of the biggest challenges while considering the extremely high cost and complex chemical process in preparation of the functionalization HNTs.

To our best knowledge, the reports on the amino epoxy nanodielectrics with the high thermal conductive and high impact strength are absent in the open literature up to now. Therefore, it is necessary to prepare the amino epoxy nanodielectrics with high thermal conductive and impact strength. The present study focus on the agglomeration of the functionalized HNTs and the interfacial interactions with epoxy resins. In this article, HNTs were treated with a silane-coupling agent (glycidoxypropyltrimethoxysilane) and were in-situ grafted by the benzidine and 4, 4'-(1, 1'-biphenyl-4, 4'-diyidioxy) dianiline (BDDA), respectively. Here, we report that epoxy/in-situ grafted HNTs nanodielectrics exhibit higher thermal conductivity, impact strength, and glass transition temperature with simultaneously significantly enhancing dielectric properties, it is possible to provide an effective low cost way of the mass production for high performance epoxy nanodielectrics in term of quantity and quality.

2. **Experimental**

2.1 Materials

Halloysite nanotubes (HNTs) were purchased from Anhui Estone Materials Technology Co., ltd, Ethanol (98%), these nanotubes were mainly tubular shapes with a length of 100 nm-1600 nm and a diameter of approximately 10-80 nm (Fig.

S1). benzidine and 4, 4'-(1, 1'-biphenyl-4, 4'-diyidioxy)dianiline (BDDA) were bought from Aladdin Chemistry Inc. Glycidoxypropyltrimethoxysilane (KH 560) and Diaminodiphenyl methane (DDM) were both acquired from Guangzhou Lunliqi synthetic resins co., Ltd. The chemical structure of the amino epoxy resin was showed in Fig. 1. All materials were not purified further due to simulating the industrial process.

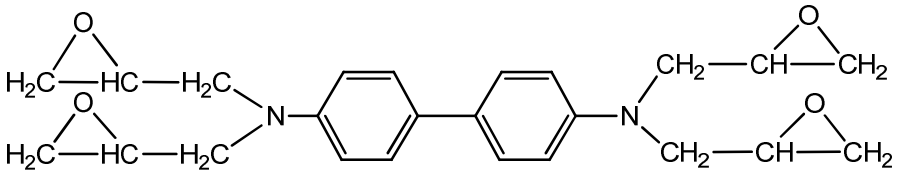

Fig. 1 The chemical structure of the amino epoxy resin.

2.2 Preparation of in-situ grafted HNTs

The 20 g of halloysite was added into a three-neck flask with a stirrer and reflux condensers, the flask was protected by nitrogen, and the three-neck flask was put in the thermostat oil bath pot. 0.2 g KH 560 was added in dropping funnel and was dropped completely within 30 minutes when the temperature reaches to 120 °C. The reaction time continued for 120 minutes. The product was named p-HNTs after cooling to room temperature. The stoichiometry benzidine and BDDA have been putted in p-HNTs for 60 minutes when the oil temperature is 130 °C, the products were named b-HNTs and d-HNTs respectively. All products were not purified further

before preparing epoxy nanodielectrics. While, the samples of HNTs, p-HNTs, b-HNTs and d-HNTs used for further characterization are dispersed in ethanol, and the mixtures were centrifuged, this cycle was repeated three times, the samples were dried under vacuum at 60 °C for 24 hours. The roughly process of the in-situ grafted HNTs was shown in Scheme 1.

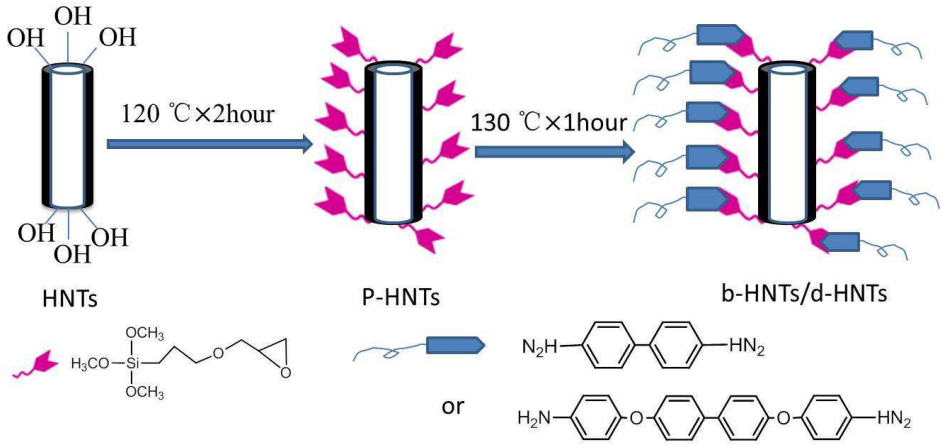

Scheme 1 Schematic representation for the in-situ grafted HNTs.

2.3 Preparation of epoxy nanodielectrics

10 g amino epoxy resin (benidine) and 3 g DDM were added into a 50 mL beaker, and the mixture was stirred by the homo-mixer for 10 minutes at 100 °C. Then 19.5 g HNTs was gradually added to the epoxy matrix and stirred continuously until the mixtures being homogeneous. The ternary mixtures were poured into the different molds and cured in an oven at 80 °C for 120 minutes and at 145 °C for 12 hours. Then, the samples were polished suitably for further testing.

2.4 Characterization

The chemical structure of HNTs and in-situ grafted HNTs were characterized by Fourier-transforms infrared spectroscopy (FTIR) with a Perkin-Elmer Paragon1000 instrument and the nuclear magnetic resonance (1H NMR) measurement with a Varian mercury plus-400 spectrometer. Surface area (BET) isotherms were obtained at the liquid nitrogen temperature of 77 K using a Micrometrics ASAP 2010 M+C. X-ray diffraction (XRD) patterns were collected on a powder diffract meter (D/max-2200/PC, Rigaku, Japan). Field emission scanning electron microscopy (FE-SEM, JSM-7401F, JEOL Ltd., Japan) was used to observe the morphology of HNTs and the fractured surfaces of epoxy nanodielectrics. Transmission electron microscopy (TEM, JEM-2100, JEOL Ltd., Japan) was performed to observe the morphology of HNTs. Thermo gravimetric analysis (TGA) was carried out with the NETZSCH TG 209 F3. Dynamic mechanical thermal analysis (DMTA) was performed on a TA Instruments DMA Q 800 equipped with a liquid nitrogen apparatus in a single cantilever mode. The thermal conductivity (λ, W m^{-1} K^{-1}) of bulk specimens was calculated by the following equation:

$$\lambda=\delta\times\rho\times Cp \quad (1)$$

Here, thermal diffusivity values (δ, mm^2 s^{-1}) were measured by laser flash method (NETZSCH LFA 447), and specific heat (Cp, J g^{-1} K^{-1}) were obtained by a

differential scanning calorimeter (DSC, 200 F3, Netzsch, Germany), bulk density (ρ) of specimens was measured with the Archimedes principle.

The universal testing machine (MTS-SANS CMT 4304, Shenzhen SANS Testing Machine Co,.Ltd) was used to measure the flexural modulus of the nanodielectrics. Charpy impact tests were determined on an impact tester (RAY-RAN Test Equipment Ltd., UK). In addition, the fracture surface of the broken specimens tested by the Charpy impact testing was examined with SEM.

The dielectric properties were measured using a Novocontrol Alpha-N high resolution dielectric analyzer (Concept 40, Germany). The AHDZ-10/100 dielectric strength tester (Shanghai Lanpotronics Co., China) was used to measure the breakdown strength of the specimens with the thickness of around 1.25 mm. A 50 Hz ramp voltage was applied across two ball typed electrodes and was increased with a rate of 2 kV s^{-1} until the sample was punctured.

3. Results and discussion

3.1 Characterization of HNTs and in-situ grafted HNTs

Fig. 2 (a) shows the FTIR spectra of HNTs and in-situ grafted HNTs. Two bands at about 3600 cm^{-1} and a single band at about 900 cm^{-1} of the spectrum were attributed to Al_2OH stretching and bending absorption, respectively. The spectrum of HNTs showed the Si-O-Si stretching bands at about 1000 cm^{-1}.[31] The peaks at about 3600

cm^{-1} of p-HNTS, b-HNTs and d-HNTs spectrums became strong, which were assigned to the Si-OH and CH–OH stretching absorption. The FTIR spectrum of b-HNTs and d-HNTs clearly showed two extensive absorption peaks at 1250-1600 cm^{-1}, which were possibly attributed to the NH scissoring vibration and Ar-NH-Ar stretching absorption.

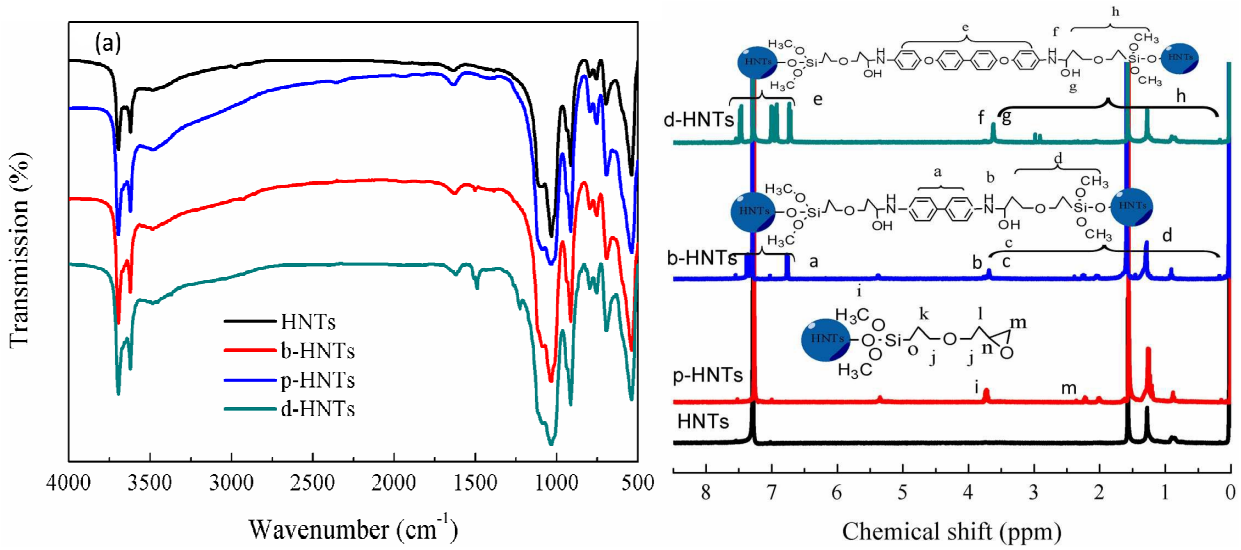

Fig. 2 FTIR and ^{1}HNMR spectra of HNTs and in-situ grafted HNTs.

The HNTs and in-situ grafted HNTs were further studied by ^{1}HNMR showed in Fig. 2 (b). The resonance at 2.38 ppm and 3.75 ppm were assigned to i and m signals of p-HNTs, the a-signals and e-signals were ascribed to the resonance of aromatic rings of b-HNTs and d-HNTs. Whereas the peaks at 0.2 ppm, 0.9 ppm, 1.3 ppm, 7.0 ppm and 7.6 ppm were present in all HNTs, it was possible that the original HNTs carried some chemicals during producing. Nevertheless, the characteristic resonance of

p-HNTs, b-HNTs and d-HNTs provided more directly evidences to obtain the in-situ grafted HNTs successfully.

3.2 Thermal stability of HNTs and in-situ grafted HNTs

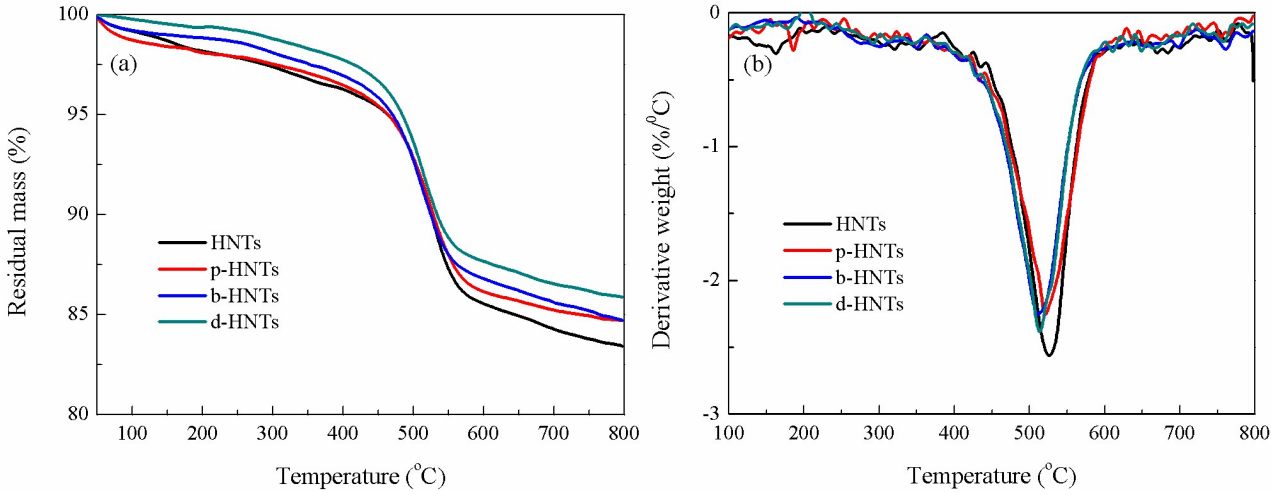

Fig.3 TG and DTG curves of HNTs and in-situ grafted HNTs.

Table 1 Characteristics thermal parameters of HNTs and In-situ grafted HNTs

Materials	HNTs	p-HNTs	b-HNTs	d-HNTs
$T_{5\%}$（°C）	480.6	472.6	459.6	464.6
$T_{50\%}$（°C）	520.8	520.3	506.0	511.6
T_{max}（°C）	560.6	567.2	554.6	560.1
Residue（%）	83.4	84.7	84.7	85.9

To determine the chemicals on the surface of in-situ HNTs, the thermo gravimetric analysis (TGA) measurements were carried out. Fig. 3 shows TG and DTG curves of

HNTs and in-situ grafted HNTs, respectively. Table 1 shows the characteristic thermal decomposition data of HNTs and in-situ grafted HNTs based on TG curves, such as temperature at 5% weight loss ($T_{5\%}$), temperature at 50% weight loss ($T_{50\%}$), temperature at maximum weight loss rate (T_{max}) and char yields at 800 °C. It was clearly visible in Fig. 3 and Table 1 that the temperature of $T_{5\%}$, $T_{50\%}$ and T_{max} of in-situ grafted HNTs were a little lower than that of HNTs and the $T_{5\%}$ of p-HNTs is the highest value of among in-situ grafted HNTs. It ascertained that the lowest chemicals on the p-HNTs exhibited the better thermal stability, b-HNTs shows a lower $T_{5\%}$ due to higher chemicals on the HNTs, whereas the $T_{5\%}$ of d-HNTs is higher than b-HNTs because the thermal stability of BDDA might be better than benzidine. Fig. 3 and Table 1 also shows that the residues of in-situ grafted HNTs were a little higher than that of HNTs. This TGA analysis is in not completely consistence with earlier reported results: the lower residues of the functionalization HNTs, the major weight loss at around 531 °C attributed to dehydroxylation of the residual structural Al-OH groups, the much lower temperatures of begins to and ends decompose of the functionalization HNTs. [31, 34] The higher residues of the functionalization HNTs in this study was attributed to the following possible reasons, the first reason was that the water of hydration in the hole of HNTs was dehydrated during HNTs grafting, and the sprays in a three-neck flask during grafting were the directly evident, the second reason was that the chemicals intercalated into the hole

of HNTs and reacted with the -OH groups on the inside wall of HNTs, the third reason was the lower percentage of grafting, the two reasons in front had a great impact on the residues of the functionalization HNTs and results in the higher residues. The major weight loss at around 560 °C was attributed to the different residual structural of Al-OH groups.

3.3 XRD analysis

X-ray diffraction analysis of HNTs and in-situ grafted HNTs was conducted and showed in Fig. 4. The basal spacing [001] of the HNTs was approximately 7.4 Å and there was a tiny peak in 10 Å, the results indicated that most of the HNTs partials used in this study were dehydrated (7.4 Å), with a small amount of hydrated particles (10Å). The result is same as that obtained by the former studies[29, 35]. As shown in Fig. 4, the in-situ grafted HNTs resulted in slightly shifting of the 7.4 Å peak to left side, corresponding to a large increment of the basal spacing, and this can be attributed to the chemical intercalating between the already dehydrated HNTs particles and further dehydration during the process of the chemical treatment. The results in this study were not consistent with that obtained by previous studies[29], probably due to higher temperature during in-situ grafting process. The chemical treatment did not result in shifting of the 10 Å peak to left side, with a small reduction of the 10 Å peaks, this can be explained that that these chemicals were unable to intercalate the hydration HNTs, on the contrary, they resulted in further

dehydration of the HNTs. The most amusing phenomenon was that the d-HNTs had the most hydration HNTs particles, which provided the direct evidence to the higher residues of in-situ HNTs.

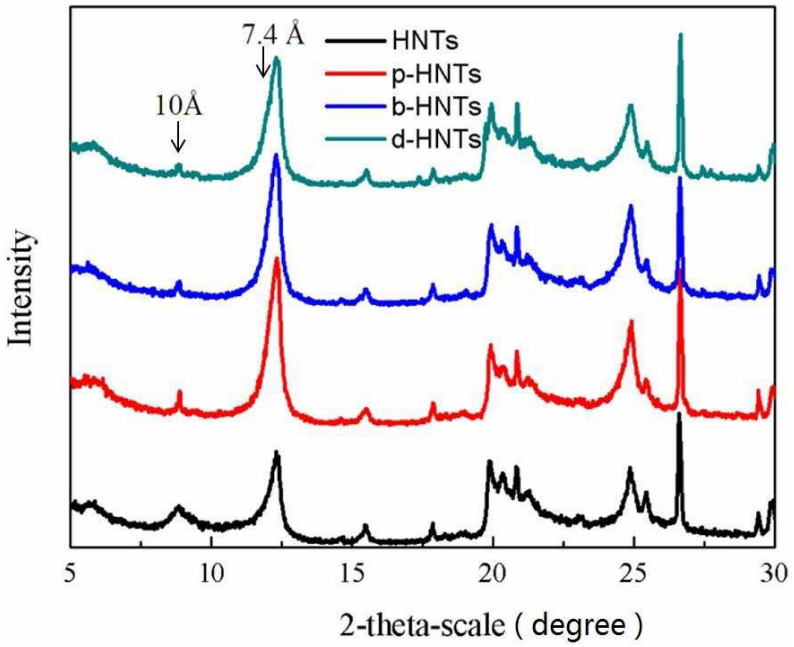

Fig. 4 XRD patterns of HNTs and in-situ grafted HNTs.

3.4 Morphology of HNTs and in-situ grafted HNTs

The morphology of HNTs and in-situ grafted HNTs is showed in Fig. 5. As it can be seen in Fig. 5, the HNTs tended to aggregate together forming clusters, while the in-situ grafted HNTs with different chemicals had a better dispersion, less agglomeration and the small particle sizes. The result showed that the chemical treatments by the in-situ method improved particle dispersion of the HNTs.

The element percentage of HNTs and in-situ grafted HNTs from SEM images accompanying EDX spectra is shown in Table 2. The average relative percentage of

carbon increased from 1.63 % to 5.36 %, and the percentage of nitrogen for b-HNTs and d-HNTs were detected to about 2.6%. The average relative percentages of aluminum and silicon of p-HNTs were higher than that of HNTs, while the ones of b-HNTs and d-HNTs were deceased. The results proved that KH 560, benzidine and BDDA were successfully grafted to the surface of HNTs.

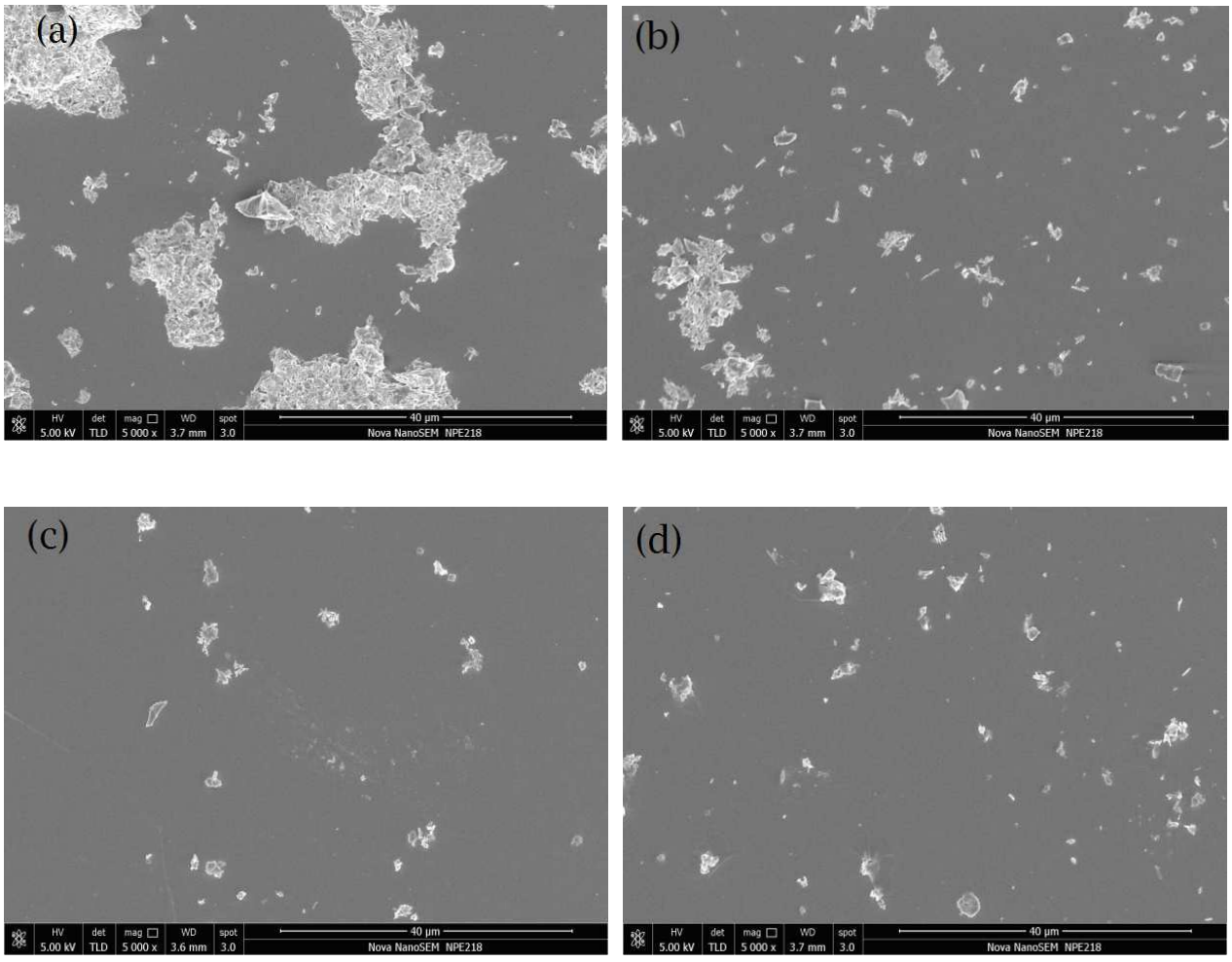

Fig.5 SEM images of HNTs :(a) HNTs, (b): p-HNTs, (c): b-HNTs, (d) d-HNTs.

Table 2 Element percentage of HNTs and in-situ grafted HNTs from SEM images accompanying EDX spectra

Element (Wt. %)	Al	Si	C	O	N	Total
HNTs	25.31	28.11	1.63	38.49	0	93.54
p-HNTs	25.82	30.39	2.06	38.60	0	96.87
b-HNTs	25.07	29.09	3.18	36.88	2.60	96.82
d-HNTs	22.25	28.39	5.36	37.90	2.58	96.48

3.5 BET analysis

Table 3 Pore structure parameters of HNTs and in-situ grafted HNTs

Name	BET surface area (m2/g)	Average pore diameter (nm)	Total pore volume (cm3/g)
HNTs	3.01	15.8	0.012
p-HNTs	29.46	16.6	0.122
b-HNTs	22.81	19.8	0.113
d-HNTs	26.91	17.5	0.118

Fig. S2 and Fig. S3 show nitrogen adsorption-desorption isotherms, pore-size distribution and t-plot curves of HNTs and in-situ grafted HNTs, the typical parameters were summarized in Table 3. The pore structure parameters of HNTs and in-situ grafted HNTs provided the directly evidence that the in-situ grafted HNTs revealed the higher BET surface area, pore volume and average pore diameter.

These results could be attributed to less agglomeration, and it was consistent with the SEM images and EDX data. The increased surface area was expected to provide stronger interaction between polymers and nanotubes.

3.6 Morphology of epoxy nanodielectrics

SEM were used to observe the morphology of the fracture surface of epoxy nanodielectrics after impact testing, the SEM images are shown in Fig. 6. As revealed in Fig. 6 (b), p-HNTs were well dispersed in the epoxy matrix with a much rougher surface, and many nanotubes were observed on the fracture surface. While, it could be seen in Fig. 6 (c) and (d) that much more cracking deflection, crack twisting and plastic deformation were observed in the fracture surface of epoxy/b-HNTs and epoxy/d-HNTs nanodielectrics.

Several toughening mechanisms for rigid inorganic particle-filled epoxies have been proposed, including: (a) an increase in fracture surface area by crack deflection and crack twisting around particles; (b) an enhancement in plastic deformation of the epoxy around particles; (c) crack front pinning by rigid particles.[37] This observation suggested that the adhesion between the in-situ grafted HNTs and the epoxy matrix was quite stronger than that between the HNTs and the epoxy matrix, and it seemed that the crack deflection, crack twisting and plastic deformation were formed in the in-situ grafted epoxy/HNTs nanodielectrics.

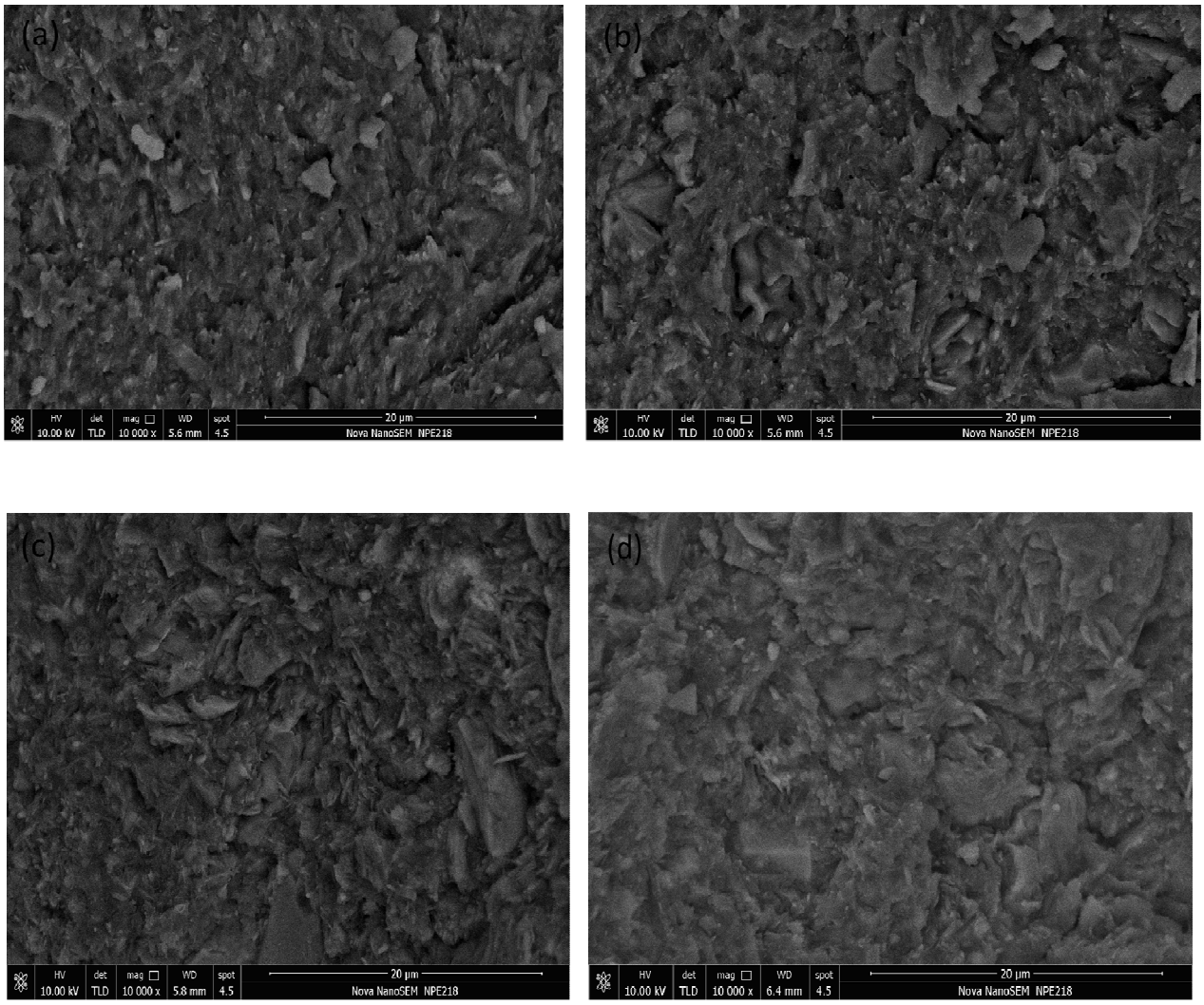

Fig. 6 SEM micrographs of epoxy nanodielectrics: (a) HNTs, (b): p-HNTs, (c): b-HNTs, (d) d-HNTs.

3.7 Dynamic mechanical behavior of epoxy nanodielectrics

Storage modulus indicates an important property to assess the loading bearing capacity of the nanodielectrics materials, and loss modulus measures the dissipated energy under deformation. Loss tangent depends on the value of loss modulus and storage modulus, and it is expressed as a damping factor being very sensitive to any

phase transformation. The glass transition temperature (T_g) is defined as the temperature which the loss tangent is up to its maximum value.[38] Fig. 7 shows the storage modulus, loss modulus and loss tangent of the Epoxy/HNTs as the function of temperature. Apparently, as shown in Fig. 7 (a), the storage modulus of epoxy/d-HNTs was the highest among the four samples at temperatures below T_g. As shown in Table 4, the introduction of d-HNTs leaded to a 28.4% increment in the storage modulus at 50 °C, the results was probably attributed to the better dispersion and stronger interface of in-situ grafted HNTs. The introduction of all in-situ grafted HNTs leaded to dramatic increment of the storage modulus when the temperature approaching its glass transition region, and the storage modulus of epoxy/b-HNTs was the highest one, up to 33% at 300 °C. The improvement could be ascribed to the tube-shape HNTs, which restrained the mobility of epoxy network as the nanosheets. It could be found that the b-HNTs had the best restraining effect on the motions of the epoxy network, and the epoxy/b-HNTs had better property to keep the loading bearing capacity around and over the glass transition region.

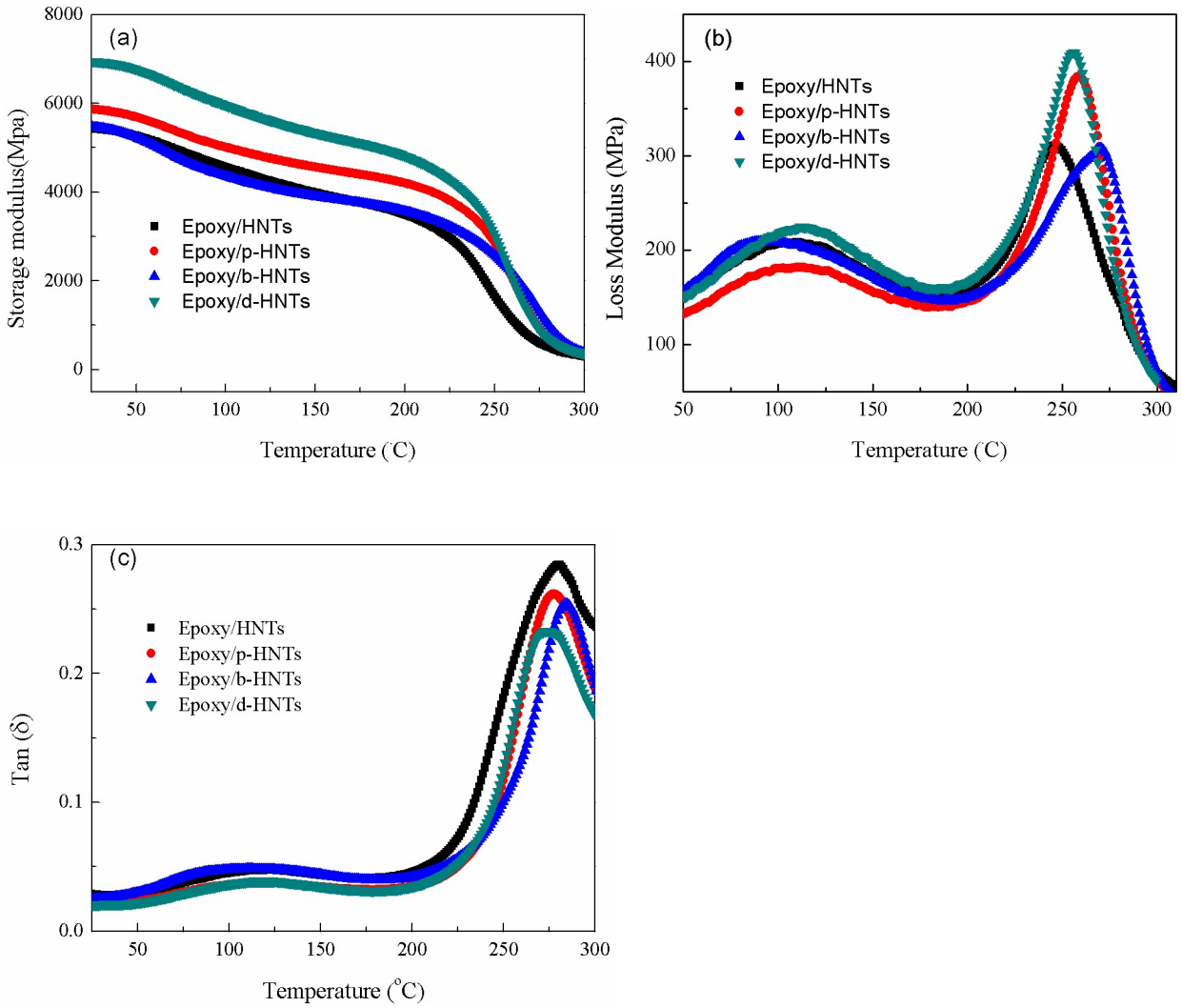

Fig. 7 Dynamic mechanical spectra of epoxy nanodielectrics: (a) Storage modulus, (b) Loss Modulus and (c) Tan δ.

Fig. 7 (b) illustrates the loss modulus for epoxy/HNTs with variation of temperature. The loss modulus values of epoxy/in-situ grafted HNTs in the transition region were much high compared to epoxy/ HNTs, the highest loss modulus value of epoxy/d-HNTs was attributed to the longer chemical trains between HNTs and epoxy matrix, the longer chemical trains increased internal friction of the epoxy

nanodielectrics and resulted in enhancing the energy dissipation [40]. While the higher loss modulus value of epoxy/p-HNTs was attributed to the better dispersion of p-HNTs in epoxy matrix.

Table 4 Storage modulus and glass transition temperature of epoxy nanodielectrics

Materials	Storage modulus(50°C)	Storage modulus(300°C)	Tg
Epoxy/HNTs	5267.9	298.8	279.7
Epoxy/p-HNTs	5684.4	334.6	277.8
Epoxy/b-HNTs	5218.3	397.3	284.3
Epoxy/d-HNTs	6762.7	375.4	273.8

As shown in Fig. 7 (c) and Table 4, the T_g values of epoxy nanodielectrics were very close, the performance was suggested to similar network characteristics. However, the peak values of T_g of epoxy/in-situ grafted HNTs were lower than that of epoxy/HNTs, and the peak values of T_g of the epoxy/b-HNTs nanodielectrics was the lowest one. This reduction could be ascribed to the higher hydroxyl group density on the external surface of in-situ grafted HNTs. The result was consistent with that of XRD analysis.

3.8 Thermal stability of epoxy nanodielectrics

Fig. 8 and Table 5 represent TG, DTG curves and Characteristics thermal parameters of epoxy nanodielectrics. The TGA curves of epoxy/ in-situ grafted HNTs

nanodielectrics did not show the similar decomposition profiles at about 320 °C as the epoxy/HNTs nanodielectrics. The in-situ grafted HNTs enhanced the initial thermal decomposition temperatures ($T_{5\%}$) and the residue at 800 °C of the nanodielectrics increased about 10 °C and 1% in compassion with the pristine HNTs, respectively. While 50% maximum thermal decomposition temperatures ($T_{50\%}$) and maximum thermal decomposition temperatures (T_{max}) were not reduced. The epoxy/b-HNTs nanodielectrics showed the highest thermal stability among all epoxy nanodielectrics. The different decomposition profiles of the epoxy/ in-situ grafted HNTs nanodielectrics may be attributed to the increased interaction between in-situ grafted HNTs and epoxy matrix and better dispersion of the in-situ grafted HNTs in epoxy matrix, which may result in retarding the permeation of volatile gas out of the epoxy nanodielectrics during thermal decomposition. [41-42]

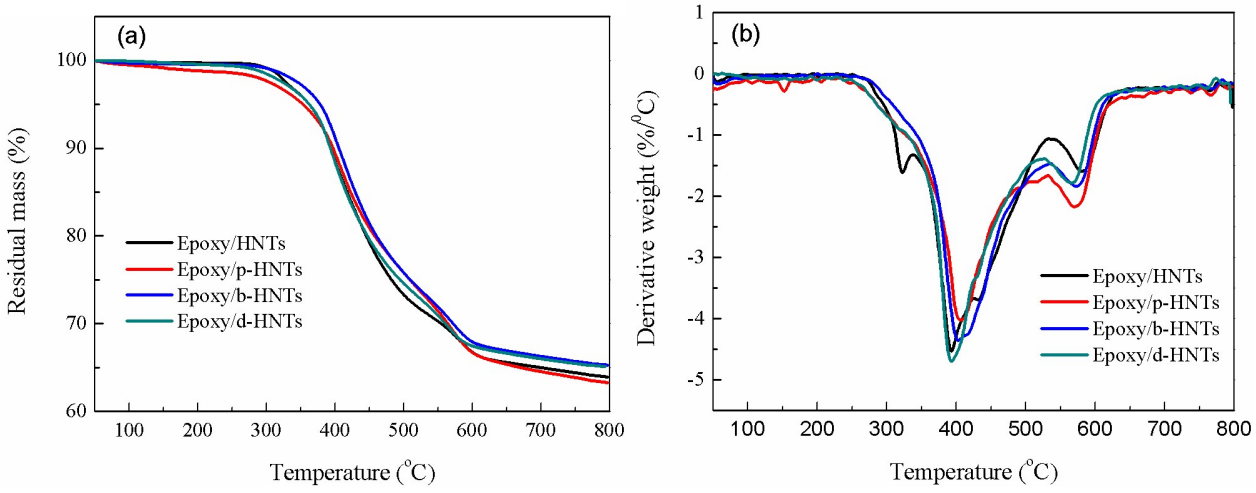

Fig. 8 TG and DTG curves of epoxy nanodielectrics: (a) TG curves; (b) DTG curves.

Table 5 Characteristics thermal parameters of epoxy nanodielectrics

Materials	Epoxy/HNTs	Epoxy/p-HNTs	Epoxy/b-HNTs	Epoxy/d-HNTs
$T_{5\%}$（°C）	345.6	353.2	355.3	353.7
$T_{50\%}$（°C）	423.8	432.6	427.9	424.0
T_{max}（°C）	506.2	515.4	504.8	496.5
Residue（%）	63.9	63.2	65.2	65.1

3.9 Mechanical property of epoxy nanodielectrics

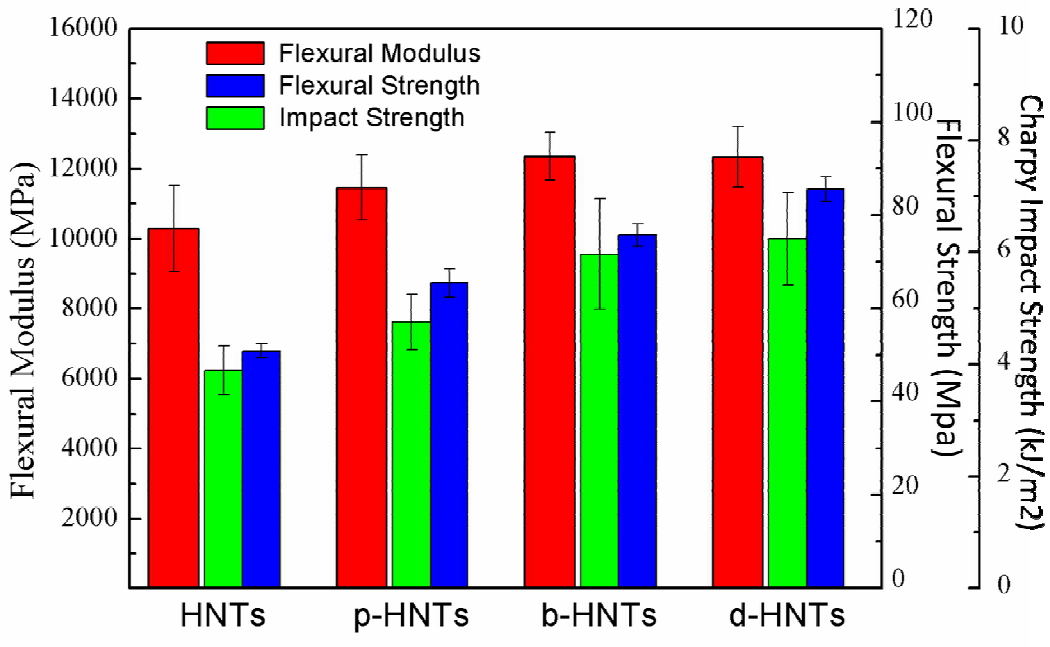

Fig. 9 Mechanical properties of epoxy nanodielectrics.

Fig. 9 represents flexural modulus, flexural strength and impact strength of the epoxy/in-situ grafted HNT nanodielectrics. Comparing with that of HNTs

nanodielectrics, the impact strength of the p-HNTs, b-HNTs and d-HNTs nanodielectrics are increased by 22.3%, 53.4% and 60.6%, respectively. Although, the improvement is not comparable to the achievement of much lower HNTs loading, [22] such largely improvement was similar with the toughness effect of rubber.[39] To our surprise, the flexural modulus, flexural strength and impact strength of the epoxy nanodielectrics were simultaneously increased by adding in-situ grafted HNTs into the epoxy matrix. The two critical factors of the uniform dispersion and interfacial compatibility were two big challenges in fabricating high performance epoxy/HNTs nanodielectrics.[11] The functionalition of HNTs was reported to the easy way in designing the interfacial interaction between HNTs and the epoxy matrix.[32] In this study, the improvement of flexural modulus, flexural strength and impact strength of the epoxy/in-situ grafted HNTs nanodielectrics was attributed to the better particle dispersion and the covalent bonding between HNTs and epoxy matrix.

3.10 Thermal property of epoxy nanodielectrics

Thermal conductivity of epoxy/HNTs nanodielectrics is shown in Fig.10. The thermal conductivity of epoxy/in-situ grafted HNTs nanodielectrics was higher than that of epoxy/HNTs nanodielectrics. To our surprise, the thermal conductivity of the epoxy/ b-HNTs nanodielectrics showed the highest value up to about 0.85 W/(m · K), about 30% higher than that the epoxy/HNTs nanodielectrics. This improvement

could be ascribed to the presence of better dispersed in-situ grafted HNTs in epoxy matrix and stronger interface between in-situ grafted HNTs and epoxy matrix.

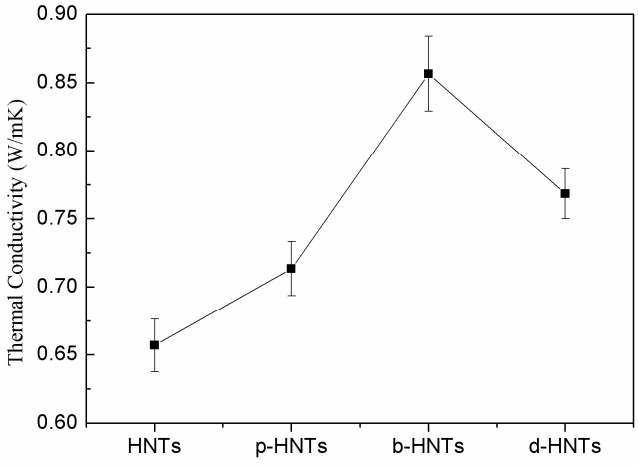

Fig. 10 Thermal conductivity of epoxy nanodielectrics.

3.11 Dielectric properties of epoxy nanodielectrics

The dielectric properties of epoxy nanodielectrics were reported by the broadband dielectric spectroscopy from 1^{-1} Hz to 10^{6} Hz at room temperature. Fig. 11 (a) and (b) show the frequency dependence of dielectric constant and dielectric loss tangent of epoxy nanodielectrics, respectively. It was obviously observed that the dielectric constant and dielectric loss tangent of the epoxy/HNTs nanodielectrics were higher than those of the epoxy/in-situ grafted HNTs nanodielectrics, especially in the low frequency range from 1 Hz to 100 Hz. The interfacial polarization -Maxwell-Wagner effect was a significant characteristic for the filler/polymer nanodielectrics, [40] the free volume theory [40, 43-45] suggested that the free volume in nanodielectrics system

would seem to be the key to change the dielectric constant. The in-situ grafted HNTs have resulted in an anomalous reduction in dielectric constants of the epoxy/in-situ grafted HNTs nanodielectrics, we envisaged that the in-situ grafted HNTs reduced the free volume, voids and defects in nanodielectrics, the SEM micrographs of the epoxy nanodielectrics (Fig. 6) provided the direct evidence that there were some impairment of dipole movements at the interfaces of epoxy/ HNTs nanodielectrics. The direct current (DC) conduction, space charge migration (interfacial polarization contribution) and the movement of molecular dipoles (diploe loss) were the three distinct factors which influence the dielectric loss of dielectric materials.[46, 47] Therefore, the decreased dielectric loss tangent could be explained as that the in-situ grafted HNTs provided better interfacial adhesion to the epoxy matrix.

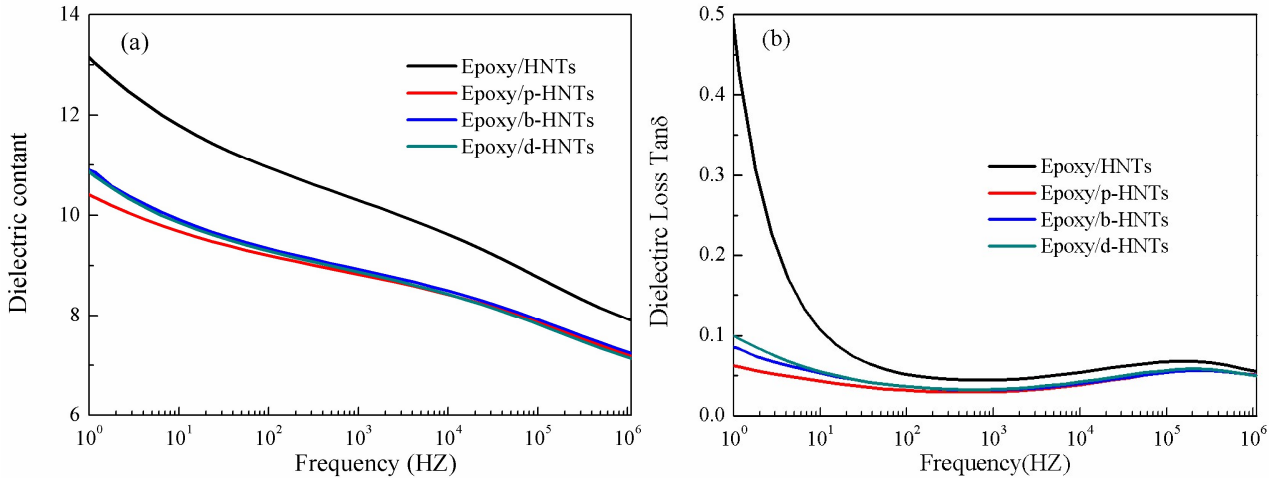

Fig. 11 Frequency dependent of dielectric properties of epoxy nanodielectrics :(a) dielectric constant, (b) dielectric Loss.

The dielectric properties of epoxy nanodielectrics under the temperature from -40 ℃ to 180 ℃ were also investigated to gain some sight on the underlying mechanisms of the dielectric properties of the epoxy/in-situ HNTs nanodielectrics at low frequency. The results are shown in Fig. S4, it could be noticed that the frequency dependence of the dielectric constants and dielectric loss Tan δof nanodielectrics were increased with temperature rising. More interestingly, the dielectric constants of epoxy/in-situ grafted HNTs nanodielectrics were much higher than that of epoxy/HNTs nanodielectrics at the low frequency with increasing of the temperature, while the dielectric loss Tan δ of all epoxy nanodielectrics showed not much difference. It was the speculation that the better interfacial adhesion reduced the free volume, voids and defects of epoxy nanodielectrics. However, the free chemicals such as KH 560, benzidine and BDDA of the in-situ grafted HNTs during in-situ grafted processing might provide the highly mobile interlayer between HNTs and epoxy matrix, the highly mobile interlayer might have the higher direct current (DC) and interfacial polarization at the higher temperature.

To clarify the influence of the free chemicals, the temperature dependent of dielectric properties of epoxy nanodielectrics at 0.1 Hz and 1 kHz were investigated and showed in Fig. S5. The results demonstrated that the dielectric constants of the epoxy/in-situ grafted HNTs nanodielectrics in 0.1 Hz was dramatically increasing with the temperature, while the dielectric constants of epoxy/HNTs nanodielectrics

in 0.1 Hz showed much stable with temperature. The dielectric loss Tan δ of all epoxy nanodielectrics at 0.1 kHz had the similar variation trend with temperature. However, the dielectric loss Tan δ on higher temperature of epoxy/in-situ grafted HNTs nanodielectrics at 1 kHz were about two times of the ones of the epoxy/HNTs nanodielectrics. Many researchers suggested that the interface in nanometer scale is one of the most important factors to determine the dielectric properties of the nanodielectric materials.[48-50] The free chemicals of the in-situ grafted HNTs in this study might not link to the surface of HNTs, its produced the highly mobile interlayer between halloysite and epoxy matrix. It was instructive to reduce the free chemicals in the in-situ grafted HNTs for improving the dielectric properties of the epoxy/in-situ grafted HNTs nanodielectrics.

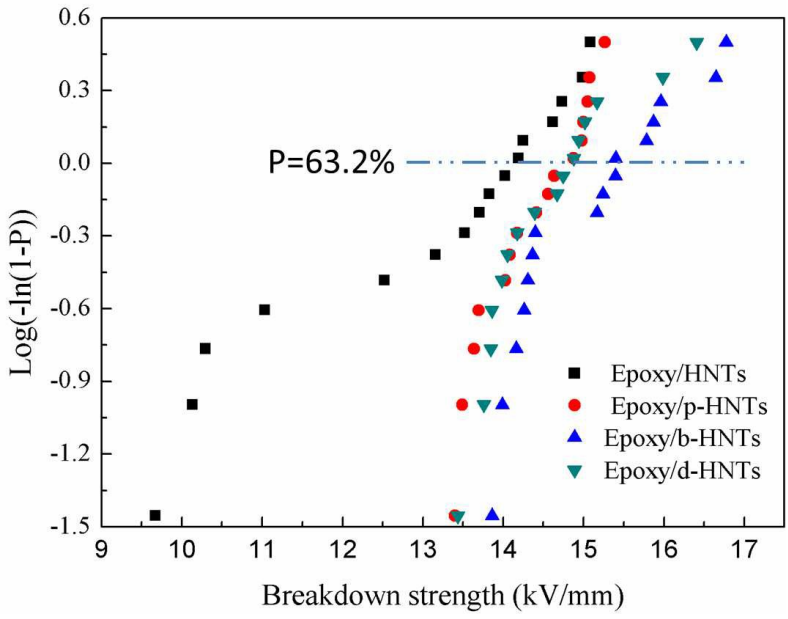

Fig.12 Weibull distribution of the breakdown strength of epoxy nanodielectrics.

Fig. 12 exhibits the Weibull distribution of the breakdown strength of epoxy nanodielectrics. It was detected from Fig. 12 that the characteristic breakdown strengths (KV/mm) of the different epoxy nanodielectrics were 13.89 kV/mm, 14.67 kV/mm, 15.49 kV/mm and 14.91 kV/mm, respectively, and the corresponding shape parameter (β) are 3.66, 12.42, 9.14 and 10.35. Both the characteristic breakdown strength and the corresponding shape parameter (β) of the epoxy/HNTs nanodielectrics show the lowest values among all epoxy nanodielectrics, the performance was attributed to the bad HNTs dispersion and some defects in epoxy/HNTs nanodielectrics.

4. Conclusions

In this paper, chemical grafting of KH 560, benzidine and BDDA onto the surface of HNTs particles were accomplished by in-situ grafting. The three functionalized HNTs were found to improve the mechanical properties, thermal properties and dielectric properties of the epoxy nanodielectrics, particularly impact strength, thermal conductivity and dielectric loss tangent. The impact strength of epoxy/b-HNTs nanodielectrics has largely increased by 53.4%. To our surprise, the flexural modulus, flexural strength and impact strength of the epoxy/in-situ grafted HNTs nanodielectrics were simultaneously increased. And the thermal conductivity of epoxy/b-HNTs nanodielectrics was up to 0.85 W m^{-1} K^{-1}, it was increased by

about 30% higher than that of epoxy/ HNTs nanodielectrics. There were also noticeable decreases in dielectric loss tangent of epoxy/b-HNTs nanodielectrics at the low frequency range from 1 Hz to 100 Hz. The results of SEM images showed that the improved physical properties of epoxy nanodielectrics may be mainly attributed to the increased interaction between in-situ grafted HNTs and epoxy matrix and better dispersion of the in-situ grafted HNTs in epoxy matrix. In summary, the epoxy thermosets/b-HNTs showed the best overall performance among all epoxy thermosets/in-situ grafting HNTs. The present epoxy/HNTs nanodielectrics with high thermal conductivity and mechanical properties offer great potential application in thermal management and next generation electronic devices.

Acknowledgments

The authors gratefully acknowledge supports from the National Science Foundation of China (Nos. 51107081, 51277117, 51477096) and the Special Fund of the National Priority Basic Research of China under Grant 2014CB239503.

Reference

1 K. S. Meenakshi, E. P. J. Sudhan, S. A. Kumar and M. J. Umapathy, *Prog. Org. Coat.,* 2012, **74**, 19.
2 Z. W. Zhou, A. J. Li, R. C. Bai and J. L. Sun, *J. Therm. Anal. Calorim. ,* 2014, **115**,1601.
3 M. Sanchez-Soto, P. Pages, T. Lacorte, K. Briceno, and F. Carrasco, *Compos. Sci. Technol.,* 2007, **67**, 1974.
4 I. Blanco, L. Oliveri, G. Cicala, A. Recca, *J. Therm. Anal. Calorim. ,* 2012, **108**, 685.
5 X. Z. Song, S. X. Zheng, J. Y. Huang, P. P. Zhu and Q. P. Guo, *J. Appl. Polym. Sci.,* 2001, **79**, 598.
6 S. J. Park, F. L. Jin and J. R. Lee, *Mater. Sci. Eng., A,* 2004, **374**, 109.
7 J. Frohlich, R. Thomann and R. Mulhaupt, *Macromolecules,* 2003, **36**,7205.

8 H. B. Gu, S. Tadakamalla, X. Zhang, Y. D. Huang, Y. Jiang, H. A. Colorado, Z. P. Luo, S. Y. Wei and Z. H. Guo, *J. Mater. Chem. C,* 2013, **1**, 729.
9 Y. C. Yuan, Y. P. Ye, M. Z. Rong, H. B. Chen, J. S. Wu, M. Q. Zhang, S. X. Qin and G. C. Yang, *Smart Mater. Struct.* ,2011, **20**, 1.
10 A. Bonnet, J. P. Pascault, H. Sautereau and Y. Camberlin, *Macromolecules,* 1999, **32**, 8524.
11 F. Hussain, M. Hojjati, M. Okamoto and R. E. Gorga, *J. Compos. Mater.,* 2006, **40**, 1511.
12 J. Njuguna, K. Pielichowski and J. R Alcock, *Adv. Eng. Mater.,* 2007, **9,** 835.
13 R. A. Vaia, G. Price, P. N. Ruth, H. T. Nguyen and J. Lichtenhan, *Appl. Clay Sci.* 1999, **15**, 67.
14 D. Ratna, and G. P. Simon, *Polymer,* 2001, **42**, 8833.
15 H. L. Mo, X. Y. Huang, F. Liu, K. Yang, S. T. li and P. K. Jiang, *IEEE Trans. Dielectr. Electr. Insul.,* 2015, **22**, 906.
16 M. Akatsuka, and Y. Takezawa, *J. Appl. Polym. Sci.,* 2003, **89**, 2464.
17 Y. X. Fu, Z. X. He, D. C. Mo and S. S. Lu, *Int. J.Therm. Sci.,* 2014, **86**, 276.
18 F. Xie, S. H. Qi, R. Yang and D. Wu, *J. Appl. Polym. Sci.,* 2015, **132**, 41255.
19 X. Y. Huang, C. Y. Zhi, P. K. Jiang, D. Golberg, Y. Bando, T. Tanaka, *Adv. Funct. Mater.,* 2013, **23**,1824.
20 V. Vahedi, P. Pasbakhsh and S. P. Chai, *Mater. Des.* 2015, **68**, 42.
21 P. Pasbakhsh,, H. Ismail, M. N. A. Fauzi and A. Abu Bakar, *Appl.Clay Sci.,* 2010, **48,** 405.
22 Y. P. Ye,, H. B. Chen, J. S. Wu and L.Ye, *Polymer*, 2007, 48, 6426.
23 S. Q. Deng,, J. D. Zhang, L. Ye, J. S. Wu, *Polymer,* 2008, **49**, 5119.
24 M. X. Liu, B. C. Guo, M. L. Du, X. J. Cai and D. M. Jia, *Nanotechnology* 2007, **18,** 455703.
25 Y. P. Ye,, H. B. Chen, J. S. Wu and C. M. Chan, *Composites Part B.,* 2011, **42**, 2145.
26 Y. P. Ye, H. B. Chen, J. S. Wu and C. M. Chan, *Compos. Sci. Technol.,* 2011, **71**,717.
27 N. Moazeni, Z. Mohamad, N. L. I. Faisal, M. A. Tehrani, and N. Dehbari, J. Appl. Polym. Sci., 2013, 130, 955.
28 S. S. Zeng, C. Reyes, J. J. Liu, P. A. Rodgers, S. H. Wentworth and L. Y. Sun, *Polymer,* 2014, **55**, 6519.
29 S. Q. Deng, J. N. Zhang and L. Ye, *Compos. Sci. Technol.,* 2009, **69**, 2497.
30 Y. H. Tang, L. Ye, S. Q. Deng, C. Yang and W. Z. Yuan, *Mater. Des.,* 2012, **42**, 471.
31 J. H. Zhang, Z. X. Jia, D. M. Jia, D. H. zhang and A. Q. Zhang, *High Perform. Polym.,* 2014, **26,** 734.
32 Y. H. Tang, S. Q. Deng, L. Ye, C. Yang, Q. Yuan, J. N. Zhang and C. B. Zhao, *Composites Part A.,* 2011, **42**, 345.
33 J. H. Zhang, D. H. Zhang, A. Q. Zhang, Z. X. Jia and D. M. Jia, *J. Plast. Compos.,* 2013, **32**, 713.
34 Yuan, P.; Southon, P. D.; Liu, Z.;Green, M. E. R.; Hook, J. M.; Antill, S. J.; Kepert, C. J. J. Phys. Chem. C. 2008, 112, 1574
35 S. R. Levis, P. B. Deasy, *Int. J. Pharm.*, 2002, **243**,17.
36 Menard KP, Dynamic Mechanical Analysis: a Practical Introduction, CRC, Boca Raton,1999.
37 A. C. Garg, Y. W. Mai, *Compos. Sci. Technol.,* 1988, **21**, 179
38 K. S. W. Sing, D. H. Evertt, R. A. W. Haul. Moscou, R.A. Pierotti, J. Rouquerol and T. Siemieniewska, *Pure Appl.Chem.,* 1985, 57,603.
39 H. Yahyaie, E. Morteza, V.T. Hamed and R. M. Ehsan, *Prog. Org. Coa.,* 2013,**76**,286.
40 R. J. Roe, *Encyclopedia of Polymer Science and Technology*, 2nd Ed, John Wiley & Sons, New York, 1987.
41 P. Sun, G. M. Liu, D. Lv, X. Dong J. S. Wu and D. J. Wang, *J. Appl. Polym. Sci.,* 2016, **13**,

2327.
42 C. H. Tseng, C. C. Wang and C. Y. Chen, *Chem. Mater.* 2007, **19** , 308.
43 J. K. Nelson, Y. Hu, *The Impact of Nanocomposite Formulations on Electrical Voltage Endurance*, 2004 International Conference on Solid Dielectrics, Toulouse, France, July, 2004.
44 S. S. Sternstein and A. J. Zhu, *Mocromelecules,* 2002, **35,** 7262.
45 O. Becker, Y. B. Cheng, R. J. Varley and G. P. Simon, *Macromolecules,* 2003, **36**, 1616.
46 A. K. Jonscher, *Nature,* 1977, **267**,673.
47 Y. Ke, X. Y. Huang, Y. H. Huang, L.Y. Xie and P. K. Jiang, *Chem. Mater.,* 2013, **25**, 2327.
48 T. J. Lewis, *IEEE Trans. Dielectr. Electr. Insul.,* 2004, **11**,739.
49 L. S. Schadler, S. K. Kumar, B. C. Benicewicz, S. L. Lewis and S. E. Harton, *MRS Bull.,* 2007, **32**, 335.
50 T. Tanaka, M. Kozako, N. Fuse and Y. Ohki, *IEEE Trans. Dielectr. Electr. Insul.,* 2005, **12**, 669.

TOC Graphic

High Thermal Conductivity and High Impact Strength of Epoxy Nanodielectrics with Functionalized Halloysite Nanotubes

Hailin Mo[a], Ke Yang[a], Shengtao Li[b] and Pingkai Jiang*[a]

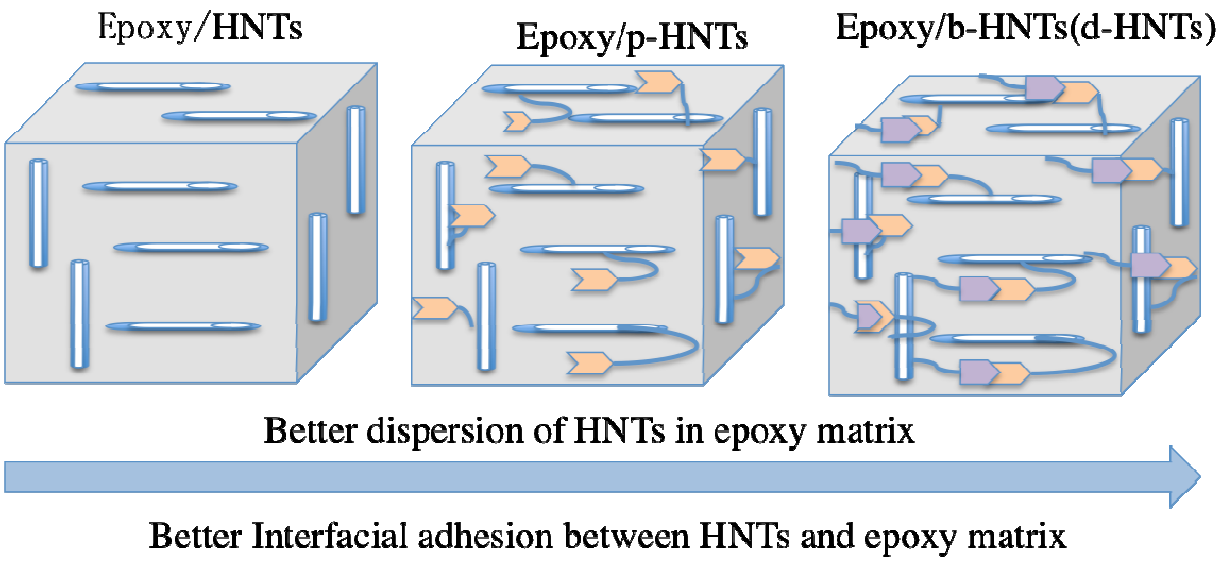

In-situ grafting HNTs were synthesized by in-situ as promising filler for epoxy nanodielectrics The resulting nanodielectrics exhibit high thermal conductivity, high impact strength and lower dielectric loss.